



## OPEN USP10 promotes cell proliferation, migration, and invasion in NSCLC through deubiquitination and stabilization of EIF4G1

Fangyi Li<sup>1,2,3</sup>, Ziyang He<sup>2,3</sup>, Xinyi Zhang<sup>1,2</sup>, Dacheng Gao<sup>2</sup>, Rui Xu<sup>2</sup>, Zhiwen Zhang<sup>2</sup>, Xingguo Cao<sup>2</sup>, Qiyuan Shan<sup>2</sup>, Yali Liu<sup>2</sup>✉ & Zengguang Xu<sup>1,2</sup>✉

Lung cancer is one of the most common types of malignant cancer worldwide, causing a serious social and economic burden. It is classified into non-small cell lung cancer (NSCLC) and small cell lung cancer, with NSCLC accounting for 80–85% of cases. Eukaryotic translation initiation factor 4 gamma 1 (EIF4G1) is highly expressed in NSCLC, playing an important role in regulating tumor growth, angiogenesis, malignant transformation, and phagocytosis. Ubiquitin-specific protease 10 (USP10) functions as a deubiquitinating enzyme to regulate substrate protein deubiquitination and reverse the ubiquitin proteasome degradation pathway. Our previous study identified an interaction between EIF4G1 and USP10; however, their regulatory mechanism remains unclear. Herein, we found that USP10 positively regulates EIF4G1 in NSCLC cells. An *in vivo* ubiquitination assay demonstrated deubiquitination of EIF4G1 by USP10, which reversed the ubiquitin proteasomal degradation of EIF4G1, thereby increasing its stability. Upregulation of EIF4G1 promoted cell proliferation, migration, and invasion in NSCLC cells. The current study not only reveals a novel mechanism through which USP10 positively regulates EIF4G1 in NSCLC, but also demonstrates the potential of USP10 as a therapeutic target to treat NSCLC.

**Keywords** Non-small cell lung cancer, USP10, EIF4G1, Tumorigenesis

Lung cancer presents a global health challenge, causing substantial social and economic burdens year-on-year. Lung cancer can be classified into two main types: non-small cell lung cancer (NSCLC) and small cell lung cancer. NSCLC accounts for approximately 80–85% of lung cancer cases<sup>1–9</sup>. In China, the incidence of new lung cancer cases continues to rise<sup>10–13</sup>. Despite advances in surgery, radiotherapy, chemotherapy, molecular targeted therapy, and immunotherapy, lung cancer remains the leading cause of cancer-related death worldwide<sup>14</sup>. Considering the much higher 5-year survival rate in patients with early-stage lung cancer than that in advanced lung cancer<sup>15</sup>, early screening and early diagnosis will play a pivotal role in improving long-term survival rates in patients with lung cancer. Thus, there is an urgent need to develop more approaches for early detection and precise treatment<sup>16–18</sup>.

Eukaryotic translation initiation factor 4 gamma 1 (EIF4G1) is a crucial component of the EIF4F complex, which consists of the m7g-cap-binding protein EIF4E, the RNA deconjugating enzyme EIF4A, and EIF4G. The EIF4F-EIF4G1 complex is essential to form the 5' cap structure of mRNA and facilitates ribosomal assembly to initiate gene translation<sup>19</sup>. Notably, EIF4G1 shows high expression levels and promotes tumor growth in several cancers, including nasopharyngeal carcinoma, inflammatory breast cancer, ovarian cancer, prostate cancer, lung cancer, and malignant pleural mesothelioma. In addition, EIF4G1 positively regulates tumor angiogenesis, malignant transformation, and phagocytosis<sup>20–25</sup>.

The ubiquitin-specific protease (USP) family is a large group of deubiquitinating enzymes containing over 50 members<sup>26,27</sup>. The *USP10* gene encodes a 798-amino acid protein that includes a substantial N-terminal region, a typical USP catalytic structural domain (approximately 380 amino acids, starting from amino acid 415), and a small C-terminal region<sup>28,29</sup>. USP10 is involved in a variety of biological processes, including DNA repair, cell cycle regulation, autophagy, and immune and inflammatory responses<sup>30,31</sup>. Increasing evidence suggests that USP10 plays a crucial role in tumorigenesis<sup>32–41</sup>. Moreover, USP10 has been identified as a novel regulator of p53.

<sup>1</sup>Shanghai East Hospital, Postgraduate Training Base of Jinzhou Medical University, Shanghai, China. <sup>2</sup>Research Center for Translational Medicine, Shanghai East Hospital, School of Medicine, Tongji University, Shanghai, China.

<sup>3</sup>Fangyi Li and Ziyang He contributed equally to this work. ✉email: yaliliuliu@163.com; xuzg1998@163.com

Knockdown of *USP10* significantly reduced the stability of p53 by increasing its ubiquitination. Accordingly, two downstream target genes of p53, *P21* and *BAX* also showed downregulation<sup>35</sup>. A negative feedback loop between *USP10* and p53 was reported. The microRNA miR-138 decreased *USP10* expression by binding to the 3'-UTR of *USP10* mRNA, but increased the expression of p53, which in turn suppressed the expression of miR-138<sup>42</sup>. Studies have shown that *USP10* can stabilize various tumor suppressors and oncogenic factors, a function that is tumor type-specific. *USP10* acts as an oncogenic factor in breast cancer, glioblastoma, and prostate cancer<sup>43,44</sup>, but serves as a cancer inhibitor in renal cell carcinoma, gastric cancer, and pancreatic cancer<sup>35,45,46</sup>.

Our previous study revealed high expression of EIF4G1 in lung cancer, functioning as an oncogenic factor by promoting tumor growth. In addition, EIF4G1 co-localized with *USP10* by binding and interacting in the cytoplasm. However, how EIF4G1 interacts with *USP10* remains unclear. The current study aimed to determine the mechanism regulating the interaction between EIF4G1 and *USP10* in lung cancer.

## Results

### Regulation of EIF4G1 expression by *USP10*

EIF4G1 functions as an oncoprotein in the development of NSCLC. *USP10* binds and interacts with EIF4G1, and these two proteins are co-localized in the cytoplasm. Immunoprecipitation experiments confirmed the interaction between EIF4G1 and *USP10* expressed either exogenously, semiexogenously, or endogenously (Fig. S1 A-C). To determine the mechanism underlying this interaction, we generated cells with stable *USP10* knockdown and analyzed the protein expression of EIF4G1, indicating a significant reduction of the EIF4G1 level in H1299, H157 and H23 cell lines with *USP10* knockdown (Fig. 1A). In addition, we examined the protein expression of EIF4G1 in H1299 cells overexpressing *USP10*, and observed elevated levels of EIF4G1 compared with that in control cells (Fig. 1B), indicating upregulation of EIF4G1 by *USP10*. For further validation, we performed rescue experiments in the *USP10*-knockdown H1299 cells by transfection them with a *USP10*-overexpressing plasmid. As expected, increased levels of EIF4G1 were observed after reexpression of *USP10* (Fig. 1C). Subsequently, we determined the change in the *EIF4G1* mRNA level with or without the expression of *USP10*. The *EIF4G1* mRNA level was reduced in *USP10*-knockdown H1299, H157, and H23 cells compared with that in control cells, suggesting that *USP10* positively regulated EIF4G1 at the transcriptional level (Fig. 1D). Furthermore, quantitative real-time reverse transcription PCR (qRT-PCR) analysis demonstrated an increased *EIF4G1* mRNA level in H1299 cells overexpressing *USP10* (Fig. 1E). These results indicated that *USP10* increases the expression of EIF4G1 protein and mRNA, and *USP10*, as a deubiquitinating enzyme, might increase the expression of EIF4G1 protein through deubiquitination.

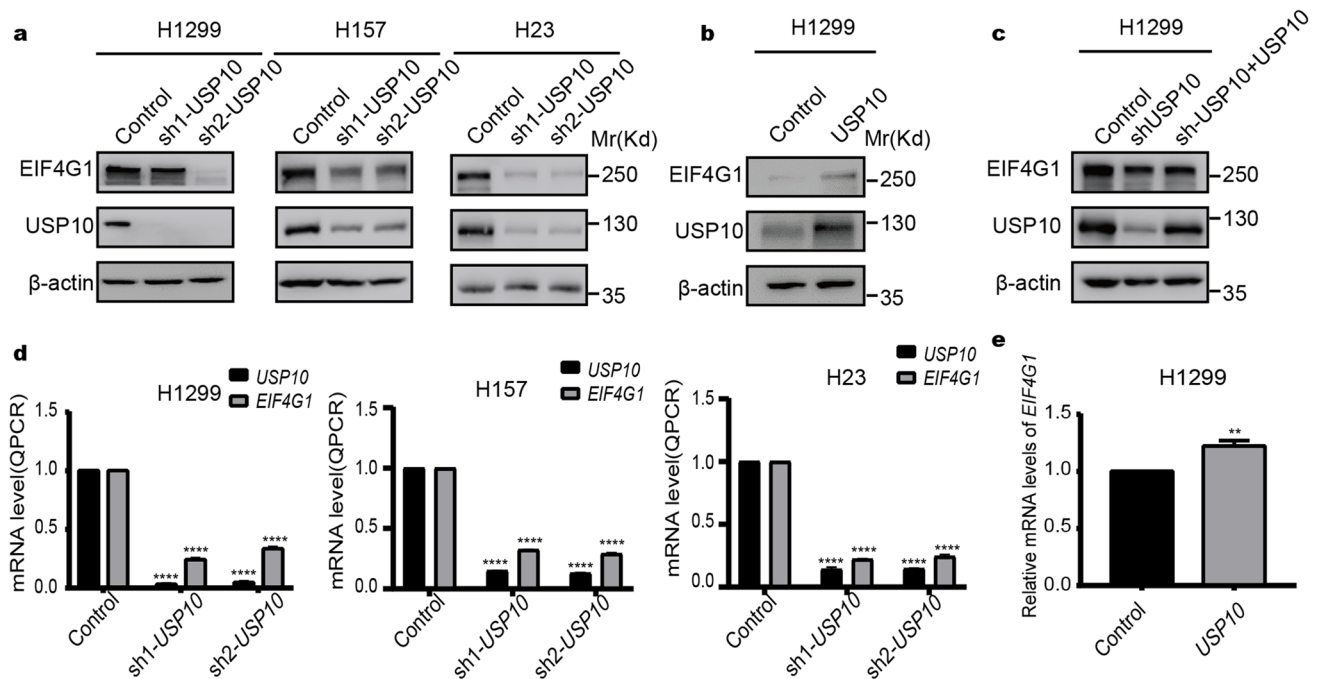


**Figure 1.** Regulation of EIF4G1 expression by *USP10*. **A** Two shRNAs downregulated the expression of *USP10* in NSCLC cell lines H1299, H157, and H23. EIF4G1 levels were detected using western blotting, with  $\beta$ -actin as the internal reference. **B** Overexpression of *USP10*. Western blotting for the protein levels of EIF4G1, with  $\beta$ -actin as the internal reference. **C** Transfection of a *USP10*-overexpressing plasmid in *USP10* knockdown H1299 cells; EIF4G1 protein levels were detected using western blotting, with  $\beta$ -actin as the internal reference. **D** Downregulation of *USP10* expression. qRT-PCR detection of the mRNA levels of *EIF4G1*, with *GAPDH* as the internal reference. **E** Overexpression of *USP10*. qRT-PCR detection of the mRNA levels of *EIF4G1*, with *GAPDH* as the internal reference. Mean  $\pm$  SD,  $n = 3$ . \*\* $P < 0.01$ , \*\*\* $P < 0.001$ , \*\*\*\* $P < 0.0001$ . Original blots are presented in Supplementary Fig. 2.

### Regulation of EIF4G1 stability by USP10

We hypothesized that USP10 stabilizes EIF4G1 through deubiquitination, leading to upregulation of EIF4G1. To test this hypothesis, we treated *USP10* knockdown H1299 cells with the protein synthesis inhibitor CHX, and analyzed the degradation rate of EIF4G1. The results showed that CHX treatment reduced the protein level of EIF4G1, but *USP10* knockdown increased the degradation rate of EIF4G1 in H1299 cells (Fig. 2A). In contrast, overexpression of *USP10* and CHX treatment in H1299 cells resulted in a slower degradation of EIF4G1 (Fig. 2B). These findings indicated that USP10 increased the stability of EIF4G1.

USP10 is a cytoplasm-specific deubiquitinating protease. Therefore, in NSCLC cells, EIF4G1 might be degraded through the ubiquitin-proteasome pathway, and USP10 might increase EIF4G1 stability by reversing this pathway. To test this hypothesis, we treated *USP10* knockdown H1299 cells with the proteasome inhibitor MG132 (10  $\mu$ M), which resulted in an increased protein level of EIF4G1 (Fig. 2C), suggesting that blocking the proteasomal degradation pathway can lead to EIF4G1 accumulation. Consequently, we concluded that USP10 increases EIF4G1 stability by suppressing its ubiquitin proteasome-mediated degradation.

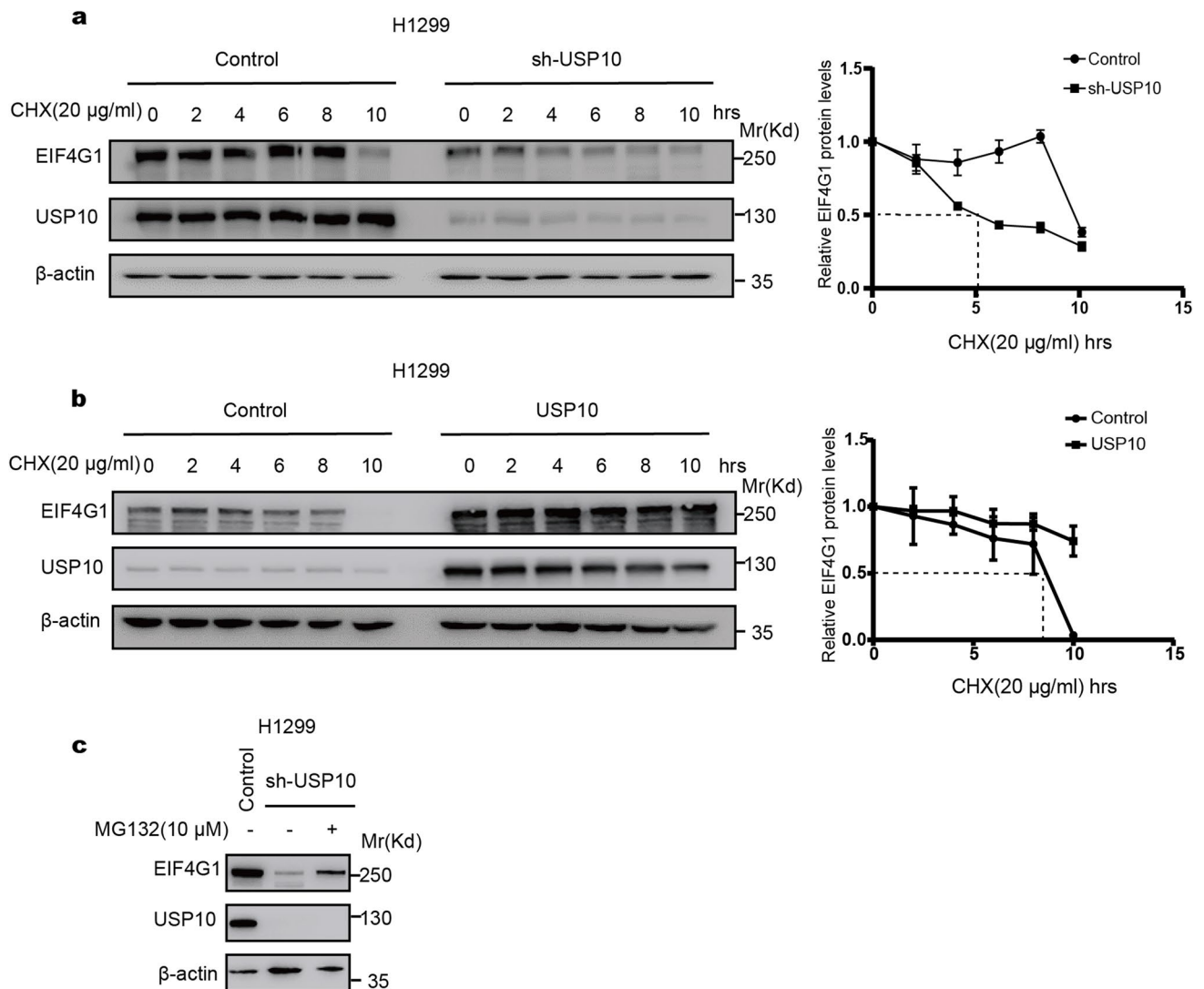


**Figure 2.** Role and pathway of USP10 in the regulation of EIF4G1 stability. **A** Control cells and H1299 cells stably knocked down for *USP10* were treated with CHX (20  $\mu$ g/mL) and harvested at the indicated times. Western blotting analysis of EIF4G1 protein levels. **B** Control cells and H1299 cells overexpressing *USP10* were treated with CHX (20  $\mu$ g/mL) and harvested at the indicated times. Western blotting was performed to analyze EIF4G1 protein levels. **C** After treating *USP10* knockdown cells with MG132 (10  $\mu$ M) for 10 h, EIF4G1 levels were detected using Western blot, with  $\beta$ -actin as the internal reference; the error bars indicate the standard deviation of three independent experiments. Mean  $\pm$  SD,  $n = 3$ . Original blots are presented in Supplementary Fig. 3.

### USP10 deubiquitylates EIF4G1

In the *USP10* knockdown 293T cells, the level of ubiquitinated EIF4G1 was significantly higher than that in the control cells (Fig. 3A). For further validation, we conducted *in vivo* ubiquitination experiments in the 293T cells stably overexpressing wild-type USP10 or USP10 C488A (USP10CA, a mutation in the core enzyme region)<sup>32</sup>. Overexpression of wild-type *USP10* significantly reduced the level of ubiquitinated EIF4G1, whereas *USP10CA* did not (Fig. 3B). These results confirmed that USP10 deubiquitinates and stabilizes EIF4G1.

### USP10 regulates NSCLC cell proliferation in an EIF4G1-dependent manner

EIF4G1 plays an important role in the development, progression, and treatment of cancer<sup>47</sup>. It is frequently overexpressed in various types of cancer, including nasopharyngeal carcinoma, squamous cell carcinoma and breast cancer<sup>21,48,49</sup>, functioning as an oncogene. To investigate whether USP10 regulates NSCLC cell proliferation by stabilizing EIF4G1, we generated NSCLC cells with stable *USP10* knockdown, *USP10* overexpression, or *EIF4G1* overexpression, respectively (Fig. S1D). CCK-8 assays showed decreased cell proliferation in the *USP10* knockdown H1299 cells compared with that in the control cells, which was rescued after overexpression of *EIF4G1* (Fig. 4A).

In addition, the proliferative ability of *USP10*-overexpressing cells was significantly higher than that of control cells (Fig. 4B), which further supported the upregulation of EIF4G1 by USP10 in H1299 cells in Fig. 1B. Similarly, clone formation assays showed fewer colonies formed by the *USP10* knockdown H1299 cells, which was rescued by *EIF4G1* overexpression (Fig. 4C). Both the number and size of the colonies formed by the *USP10*-overexpressing cells were significantly increased compared with those of the control cells (Fig. 4D). These results indicated that USP10-mediated deubiquitination of EIF4G1 increased the EIF4G1 levels and thereby promoted proliferation in NSCLC cells.

### USP10 regulates NSCLC cell migration in an EIF4G1-dependent manner

We hypothesized that USP10 might influence tumor cell migration by regulating EIF4G1 stability. To test the hypothesis, we performed wound healing assays, which revealed a significant decrease in cell migration in the *USP10* knockdown cells, compared with that of the control cells, which was rescued by *EIF4G1* overexpression (Fig. 5A). Furthermore, wound healing assays using *USP10* overexpressing cells showed a higher migration rate in H1299 cells compared with that of the control cells (Fig. 5B). The results were further validated by applying additional Transwell migration assays (Fig. 5C and D). In conclusion, USP10 promotes NSCLC cell migration in an EIF4G1-dependent manner.

### USP10 regulates NSCLC cell invasion in an EIF4G1-dependent manner

Transwell invasion assays were applied to detect the cell invasive capability. *USP10* knockdown significantly suppressed cell invasion, which was rescued by *EIF4G1* overexpression (Fig. 6A). Overexpression of *USP10* significantly promoted cell invasion (Fig. 6B). These results confirmed that USP10 promotes the invasive capacity of NSCLC cells in an EIF4G1-dependent manner.

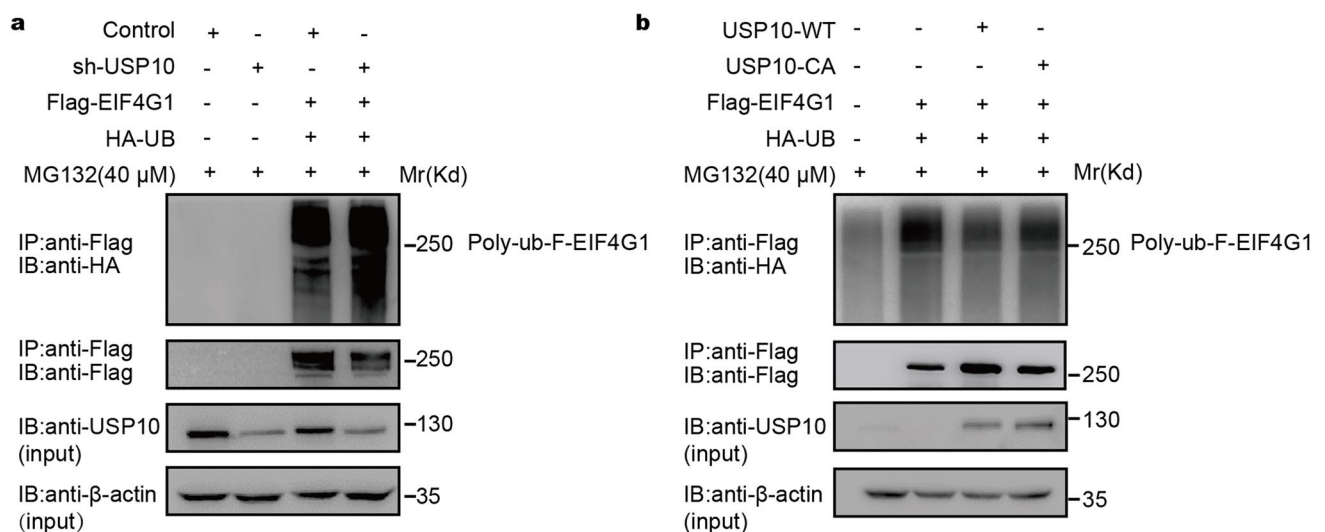


**Figure 3.** USP10 Deubiquitylated EIF4G1. **A** The EIF4G1 expression vector and HA-UB were transfected into control and *USP10* knockout cells. The cells were then treated with MG132 (40 μM) for 4 h. Immunoprecipitation was performed using FLAG beads and immunoblotting was performed as indicated. **B** The EIF4G1 expression vector and HA-UB were transfected into wild-type *USP10* and *USP10* mutant overexpressing cells. The cells were then treated with MG132 (40 μM) for 4 h, followed by immunoprecipitation using FLAG beads, and immunoblotting as indicated. Original blots are presented in Supplementary Fig. 4.

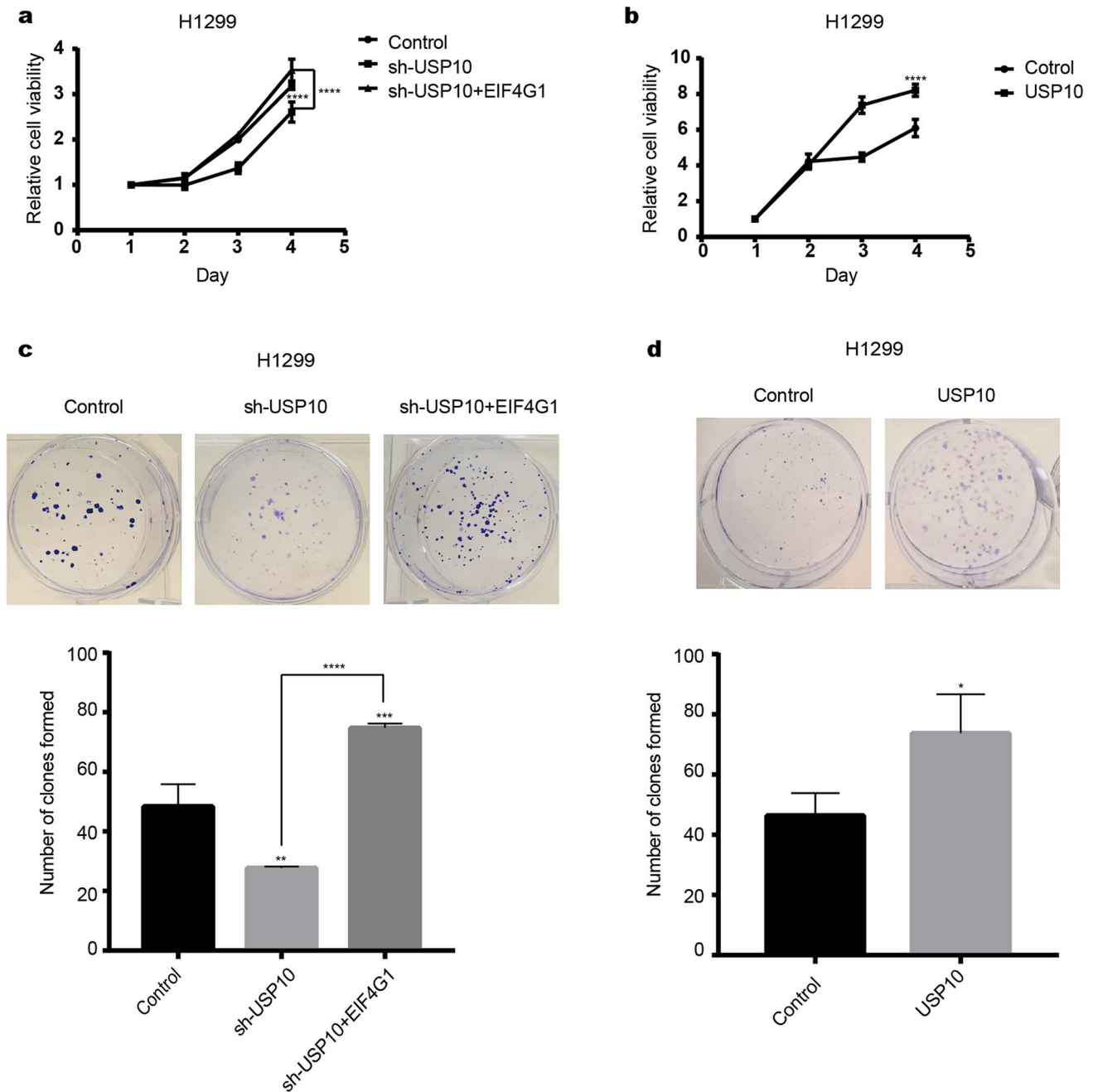


**Figure 4.** USP10 regulates non-small cell lung cancer cell proliferation in an EIF4G1-dependent manner. **A** CCK-8 assay of the proliferative capacity of control H1299 cells, *USP10* knockdown cells, and *USP10* knockdown plus *EIF4G1* overexpression cells. **B** CCK-8 assay of the proliferative capacity of cells overexpressing *USP10* and control H1299 cells. **C** Clone formation assay to detect the proliferative ability of control H1299 cells, *USP10* knockdown cells, and *USP10* knockdown plus *EIF4G1* overexpression cells. **D** Clone formation assay to detect the proliferative ability of cells overexpressing *USP10* and control H1299 cells. Mean  $\pm$  SD,  $n = 3$ . \*\* $P < 0.01$ , \*\*\* $P < 0.001$ , \*\*\*\* $P < 0.0001$ .

## Discussion

Early screening and early diagnosis are the most important means to improve the long-term survival rate of patients with lung cancer. Currently, low-dose computed tomography is regarded as an effective and promising screening method for lung cancer. However, it is limited because of a lack of malignant nodule specificity and the increased psychological and physiological burden on patients<sup>50</sup>. Liquid biopsy also shows promise as a non-invasive, accurate, and predictive tool in cancer diagnosis. The oncogene *EIF4G1* is highly expressed in tumors, promoting tumor cell proliferation. Its inhibitor, 4EGI-1, effectively suppresses gene translation in breast cancer stem cells by interacting with translation initiation factors EIF4E1 and EIF4G1<sup>51</sup>. In addition, EIF4G1 has been

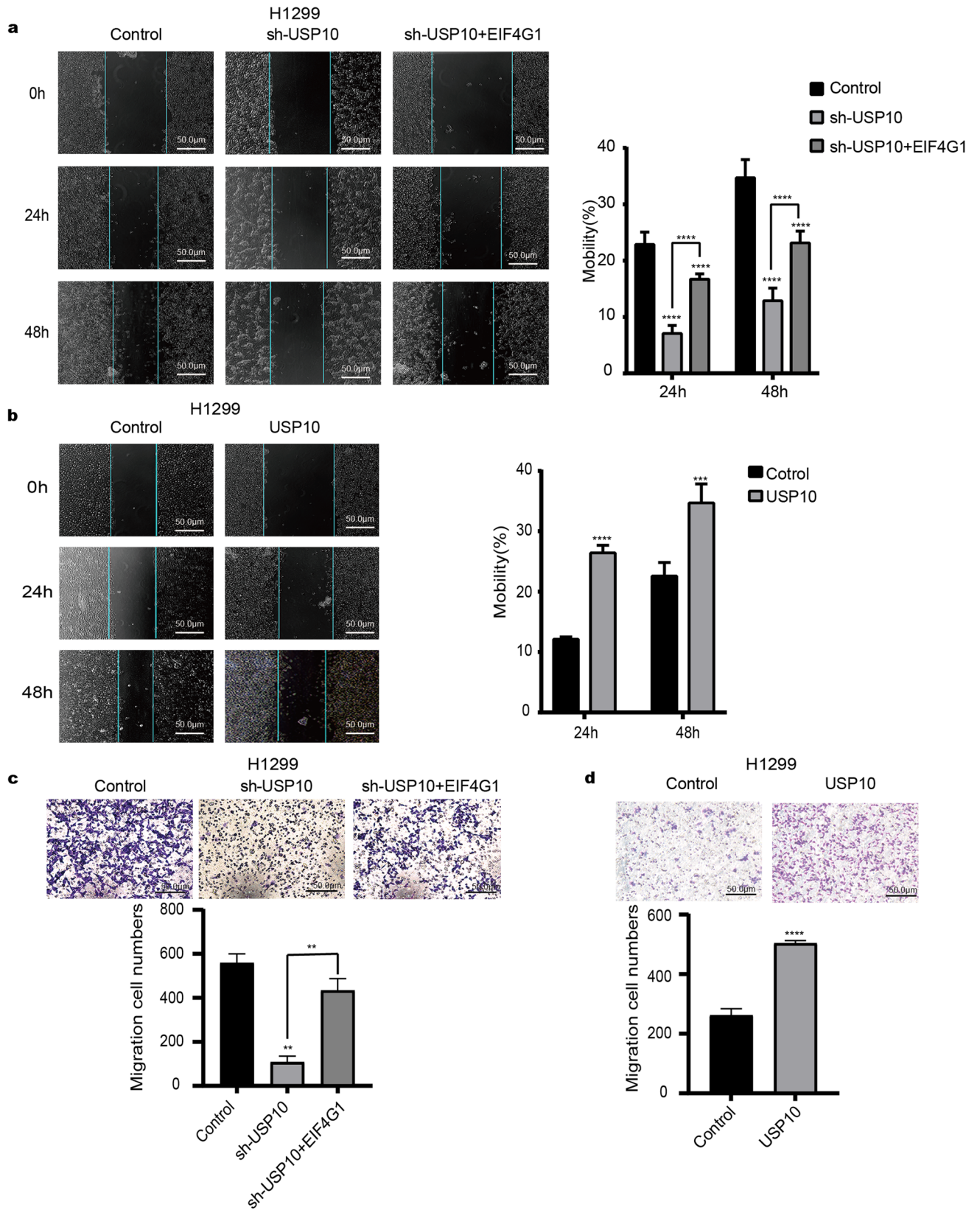


**Figure 5.** USP10 regulates non-small cell lung cancer cell migration in an EIF4G1-dependent manner. **A** Cell scratch assay for the migratory ability of control H1299 cells, USP10 knockdown cells, and USP10 knockdown plus EIF4G1 overexpression cells. **B** Cell scratch assay to detect the migration ability of cells overexpressing USP10 and control H1299 cells. **C** Transwell migration assay to detect the migration ability of control H1299 cells, USP10 knockdown cells, and USP10 knockdown plus EIF4G1 overexpression cells. **D** Transwell migration assay was performed to detect the migration ability of cells overexpressing USP10 and control H1299 cells. Mean  $\pm$  SD,  $n = 3$ . \*\* $P < 0.01$ , \*\*\* $P < 0.001$ , \*\*\*\* $P < 0.0001$ . Scale bars: 50  $\mu$ m.

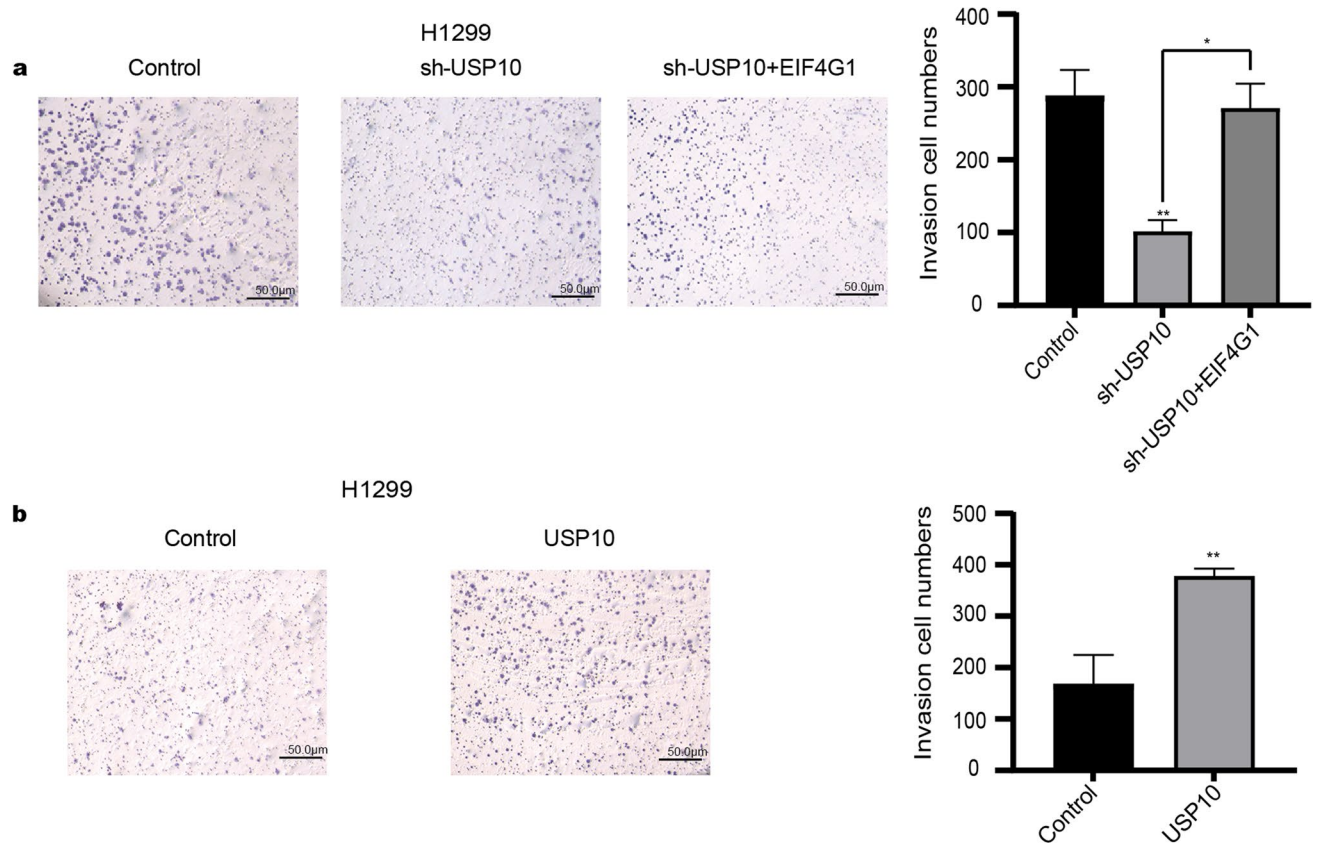


**Figure 6.** USP10 regulates non-small cell lung cancer cell invasion in an EIF4G1-dependent manner. **A** Transwell invasion assay detecting the invasion ability of control H1299 cells, *USP10* knockdown cells, and *USP10* knockdown plus *EIF4G1* overexpression cells. **B** Transwell invasion assay detecting the invasion ability of cells overexpressing *USP10* and control H1299 cells. Mean  $\pm$  SD,  $n = 3$ . \* $P < 0.5$ , \*\* $P < 0.01$ . Scale bars: 50  $\mu$ m.

reported to regulate the expression and phosphorylation of mechanistic target of rapamycin kinase (mTOR, Ser2448), thereby promoting NSCLC tumor growth<sup>24</sup>. The deubiquitinating enzyme USP10 is involved in the regulation of DNA repair, cell cycle, autophagy, and immune and inflammatory responses<sup>30,31</sup>. The Notch receptor (NOTCH) and transforming growth factor  $\beta$  (TGF- $\beta$ ) exist in different cancer species and play carcinogenic or anticancer roles. NOTCH is an oncogenic factor in leukemia, which directly activates MYC expression through NME and promotes the growth, proliferation, and self-renewal of leukemia cells<sup>52</sup>. In head and neck tumors, NOTCH can significantly block cells in the G1 phase by increasing P21 levels, thus playing a tumor suppressant role<sup>53</sup>. TGF- $\beta$  induces pleckstrin 2 (PLEK2) expression in breast cancer by activating *PLEK2* promoter activity, thus playing a carcinogenic role<sup>54</sup>. In colon cancer, TGF- $\beta$  induces Smad2/3 phosphorylation and forms a complex with Smad4 to accumulate in the nucleus. This inhibits the production of inflammatory cytokines and chemokines, thus playing a tumor suppressant role<sup>55</sup>. It has also been reported that USP10 plays a crucial role in regulating tumorigenesis, depending on the tumor type. USP10 acts as oncogene in breast cancer, glioblastoma, and prostate cancer<sup>43,44</sup>, and as a tumor suppressor in kidney, stomach, and pancreatic cancer<sup>35,45,46</sup>. Therefore, we speculated that this tumor type-specific function of USP10 might be similar to that of NOTCH and TGF- $\beta$ . Thus, there may be more complex molecular mechanisms underlying USP10' function, which requires further study and exploration.

To effectively diagnose and treat lung cancer, novel therapeutic targets need to be explored. EIF4G1 and USP10 are closely related to cancer development and progression. EIF4G1 is highly expressed in NSCLC and interacts with USP10. The literature suggests EIF4G1 and USP10 as new potential targets for lung cancer treatment. In the current study, we found that USP10 positively regulates EIF4G1. USP10 deubiquitinated EIF4G1, thereby increasing its stability. *USP10* knockdown decreased the proliferation, migration, and invasion in NSCLC cells, which were rescued by *EIF4G1* overexpression. Thus, USP10 promotes the proliferation, migration and invasion of NSCLC by increasing the level of EIF4G1, providing a new target for the treatment of lung cancer. However, further validation using animal experiments and clinical sample analysis *in vivo* are required. USP10, as a deubiquitinating enzyme, can act on a variety of substrate molecules to regulate their ubiquitination and stability, such as Yes1 associated transcriptional regulator (YAP1), Nuclear factor erythroid 2-related factor 2 (Nrf2), sirtuin6 (SIRT6), P53, MOF (also known as lysine acetyltransferase 8), and these molecules either directly affect gene transcription, affect gene transcription through antagonism, or affect histone enrichment at the promoter, thus influencing the mRNA expression level of the target gene<sup>37,56–58</sup>. We speculated that one or several USP10

substrate molecules might be involved in the regulation of *EIF4G1* mRNA expression, such that USP10 not only directly affects the stability of the EIF4G1 protein through deubiquitination, but also the expression level of *EIF4G1* mRNA is indirectly through other substrate molecules. The complex regulatory mechanism remains to be further studied.

## Methods

### Cell culture

NSCLC cell lines H1299 and HEK 293T were obtained from the Shanghai Institutes for Biological Sciences (Shanghai, China). NSCLC cell lines H157 and H23 were obtained from iCellBioscience Inc. (Shanghai, China). Cells were cultured in Dulbecco's modified Eagle's medium (Corning Inc., Corning, NY, USA) containing 10% fetal bovine serum and 1% penicillin/streptomycin (Corning Inc.).

### Western blotting

The cell lysate was extracted using Radioimmunoprecipitation assay buffer containing protease inhibitors. Protein extracts were then subjected to sodium dodecyl-sulfate polyacrylamide gel electrophoresis and transferred onto nitrocellulose membranes. The proteins on the membranes were blocked using 5% skim milk in Tris-buffered saline/Tween 20 and incubated with primary antibodies overnight at 4 °C, followed by incubation with labeled secondary antibodies. Images of the immunoreactive protein bands were acquired using the SageCapture System (Sage Creation, Beijing, China). The primary antibodies we used were: anti- $\beta$ -actin (AC026, 1:10000; ABclonal, Wuhan, China); anti-EIF4G1 (8701 S, 1:1000), anti-FLAG (2368 S, 1:1000), and anti-IgG (2729 S, 1:1000), all from Cell Signaling technology (Danvers, MA, USA); anti-HA (H3663, 1:1000, Sigma, Roedermark, Germany); and anti-USP10 (PA5-52334, 1:1000, Thermo Fisher Scientific, Waltham, MA, USA).

### Total RNA extraction and quantitative real-time reverse transcription PCR (qRT-PCR)

Total RNA was extracted using a Total RNA Isolation Reagent (SuPerfectRI, Pufei Biotech, Jiangsu, China). Reverse transcription of the RNA was performed using an ABScript III RT Master Mix for qPCR (ABclonal). The cDNA was subjected to quantitative real-time PCR analysis using ExaGreen 2X qPCR MasterMix (Applied Biological Materials Inc., Richmond, Canada) and an Applied Biosystems™ 7500 instrument (Foster City, CA, USA). The primers for *GAPDH* (control) were purchased from Sangon Biotech (Shanghai, China). Other primers used were: *EIF4G1* forward 5'-CTCTTCATCTTTGTACGGCATA-3', reverse 5'-CCTTGGTACTGAG CAGTAG-3'; *USP10* forward 5'-GGTGAAGGAAGCGAGGATGAATGG-3', reverse 5'-AATTGCCGGTGATT GGAGTCTGAAC-3'.

### Cycloheximide (CHX) protein degradation assay

Cells were cultured in medium containing 20  $\mu$ g/mL CHX (AbMole, Houston, TX, USA) at 37 °C. Cell lysates were prepared using lysis buffer every 2 h during CHX incubation.

### Immunoprecipitation assay

Proteins were extracted from cells using Radioimmunoprecipitation assay buffer with protease inhibitors on ice for 1 min. Supernatants were collected and incubated with ANTI-FLAG M2 Affinity Gel (A2220, Sigma) at 4 °C for 4 h. The beads were then washed five times using lysis buffer, and the samples were resuspended in 1% sodium dodecyl sulfate, boiled at 100 °C for 5 min, and then subjected to electrophoresis and western blotting.

### Cell Counting Kit-8 (CCK8) cell proliferation assay

Cells (1,000 cells/well) were seeded in 96-well plates and cultured for 4 days, then 10  $\mu$ L of CCK 8 reagent (ShareBio, Hangzhou, China) was added. The absorbance at 450 nm was measured after 2 h using a microplate reader (Thermo Fisher Scientific). The results were analyzed using GraphPad Prism7 (GraphPad Inc., La Jolla, CA, USA).

### Colony formation assay

Cells (1,000 cells/well) were seeded in 6-well plates, and cultured for 14 days, followed by washing with phosphate-buffered saline, fixing with methyl alcohol spirit for 10 min, and staining with crystal violet solution (Beyotime, Jiangsu, China).

### Wound healing assay

The cells were grown to full confluency in 6-well plates and then incubated overnight in starvation medium. The cell monolayer was scratched using a sterile fine pipette tip, washed with medium to remove detached cells, and the wound was photographed under a microscope. The cells were incubated for 48 h and then the wound gap was photographed under the microscope again. The difference in the size of the wound determined the wound healing rate.

### Transwell migration assay

The migration assay was performed using 6-well Transwell chambers (8  $\mu$ m, Labselect, Hefei, China). Following transfection, tumor cells were resuspended in serum-free Dulbecco's modified Eagle's medium. Then,  $1 \times 10^6$  cells were seeded into the upper chambers and 2 mL of Dulbecco's modified Eagle's medium containing 20% fetal bovine serum were added to the bottom chambers. After incubation for 48 h, the non-migrated cells were gently removed using a cotton swab. Migrated cells located on the lower side of the chamber were stained with 0.1% crystal violet (Beyotime) and counted under a microscope.



### Transwell invasion assay

The invasion assay was performed using 24-well Transwell chambers (8  $\mu\text{m}$ ; Corning Inc.). Following transfection, tumor cells were resuspended in serum-free Roswell Park Memorial Institute 1640 medium. Then,  $5 \times 10^4$  cells were seeded into the upper chambers, which were covered with Matrigel (BD Biosciences, San Jose, CA, USA), and 0.5 mL of Roswell Park Memorial Institute 1640 containing 20% fetal bovine serum was added to the bottom chambers. After incubation for 48 h, the non-invaded cells were gently removed using a cotton swab. Invaded cells located on the lower side of the chamber were stained with 0.1% crystal violet and counted under a microscope.

### RNA interference and gene overexpression

To establish stable *USP10* knockdown cells, we used short-hairpin RNAs (shRNAs) from Dharmacon (Lafayette, CO, USA): USP10-shRNA1 (KD1), USP10-shRNA2 (KD2), and a nonsilencing (NS)-shRNA as a control. To establish stable *EIF4G1* or *USP10* overexpressing cells, we transfected cells with a *USP10* overexpression plasmid, an *EIF4G1* overexpression plasmid, the USP10 mutant USP10C488A (USP10CA)-expressing plasmid, and a nonoverexpressing plasmid as a control (Ribobio, Guangzhou, China).

### Statistical analysis

The differential expression between two groups was evaluated using an independent Student's t-test in GraphPad Prism7. The results are shown as the mean  $\pm$  SD.  $p < 0.05$  was considered statistically significant.

### Data availability

All data generated or analysed during this study are included in this published article [and its supplementary information files].

Received: 22 March 2024; Accepted: 26 September 2024

Published online: 10 October 2024

### References

- Wei, W. et al. Cancer registration in China and its role in cancer prevention and control. *Lancet Oncol.* **21**, e342. [https://doi.org/10.1016/s1470-2045\(20\)30073-5](https://doi.org/10.1016/s1470-2045(20)30073-5) (2020).
- Siegel, R. L., Miller, K. D., Fuchs, H. E. & Jemal, A. Cancer statistics, 2022. *Cancer J. Clin.* **72**, 7–33. <https://doi.org/10.3322/caac.21708> (2022).
- Sung, H. et al. Global Cancer statistics 2020: GLOBOCAN estimates of incidence and Mortality Worldwide for 36 cancers in 185 countries. *Cancer J. Clin.* **71**, 209–249. <https://doi.org/10.3322/caac.21660> (2021).
- Cao, W., Chen, H. D., Yu, Y. W., Li, N. & Chen, W. Q. Changing profiles of cancer burden worldwide and in China: a secondary analysis of the global cancer statistics 2020. *Chin. Med. J.* **134**, 783–791. <https://doi.org/10.1097/cm9.0000000000001474> (2021).
- Gao, S. et al. Lung Cancer in people's Republic of China. *J. Thorac. Oncol.* **15**, 1567–1576. <https://doi.org/10.1016/j.jtho.2020.04.028> (2020).
- Zoncu, R., Efeyan, A. & Sabatini, D. M. mTOR: from growth signal integration to cancer, diabetes and ageing. *Nat. Rev. Mol. Cell Biol.* **12**, 21–35. <https://doi.org/10.1038/nrm3025> (2011).
- Chen, W. et al. Cancer statistics in China, 2015. *CA Cancer J. Clin.* **66**, 115–132. <https://doi.org/10.3322/caac.21338> (2016).
- Travis, W. D. et al. The 2015 World Health Organization Classification of Lung Tumors: impact of genetic, clinical and radiologic advances since the 2004 classification. *J. Thorac. Oncol.* **10**, 1243–1260. <https://doi.org/10.1097/jto.0000000000000630> (2015).
- Chen, P., Liu, Y., Wen, Y. & Zhou, C. Non-small cell lung cancer in China. *Cancer Commun. (London England)*. **42**, 937–970. <https://doi.org/10.1002/cac2.12359> (2022).
- Blizzard, L. & Dwyer, T. Declining lung cancer mortality of young Australian women despite increased smoking is linked to reduced cigarette 'tar' yields. *Br. J. Cancer*. **84**, 392–396. <https://doi.org/10.1054/bjoc.2000.1558> (2001).
- Qiu, H., Cao, S. & Xu, R. Cancer incidence, mortality, and burden in China: a time-trend analysis and comparison with the United States and United Kingdom based on the global epidemiological data released in 2020. *Cancer Commun. (London England)*. **41**, 1037–1048. <https://doi.org/10.1002/cac2.12197> (2021).
- Giovino, G. A. et al. Tobacco use in 3 billion individuals from 16 countries: an analysis of nationally representative cross-sectional household surveys. *Lancet (London England)*. **380**, 668–679. [https://doi.org/10.1016/s0140-6736\(12\)61085-x](https://doi.org/10.1016/s0140-6736(12)61085-x) (2012).
- Ng, M. et al. Smoking prevalence and cigarette consumption in 187 countries, 1980–2012. *JAMA* **311**, 183–192. <https://doi.org/10.1001/jama.2013.284692> (2014).
- Siegel, R. L., Miller, K. D., Jemal, A. & Cancer statistics, 2020. *CA Cancer J. Clin.* **70**, 7–30. <https://doi.org/10.3322/caac.21590> (2020).
- Goldstraw, P. et al. The IASLC Lung Cancer Staging Project: proposals for revision of the TNM Stage groupings in the Forthcoming (Eighth) Edition of the TNM classification for Lung Cancer. *J. Thorac. Oncol.* **11**, 39–51. <https://doi.org/10.1016/j.jtho.2015.09.009> (2016).
- Jett, J. R. et al. Audit of the autoantibody test, EarlyCDT<sup>+</sup>-lung, in 1600 patients: an evaluation of its performance in routine clinical practice. *Lung Cancer (Amsterdam Netherlands)* **83**, 51–55. <https://doi.org/10.1016/j.lungcan.2013.10.008> (2014).
- Wang, W. et al. The diagnostic value of a seven-autoantibody panel and a nomogram with a scoring table for predicting the risk of non-small-cell lung cancer. *Cancer Sci.* **111**, 1699–1710. <https://doi.org/10.1111/cas.14371> (2020).
- Li, C. et al. Advances in lung cancer screening and early detection. *Cancer Biol. Med.* **19**, 591–608. <https://doi.org/10.20892/j.issn.2095-3941.2021.0690> (2022).
- Haimov, O. et al. Dynamic interaction of eukaryotic initiation factor 4G1 (eIF4G1) with eIF4E and eIF1 underlies scanning-dependent and -independent translation. *Mol. Cell. Biol.* **38**. <https://doi.org/10.1128/mcb.00139-18> (2018).
- Tu, L. et al. Over-expression of eukaryotic translation initiation factor 4 gamma 1 correlates with tumor progression and poor prognosis in nasopharyngeal carcinoma. *Mol. Cancer*. **9**, 78. <https://doi.org/10.1186/1476-4598-9-78> (2010).
- Silvera, D. et al. Essential role for eIF4G1 overexpression in the pathogenesis of inflammatory breast cancer. *Nat. Cell Biol.* **11**, 903–908. <https://doi.org/10.1038/ncb1900> (2009).
- Li, L. et al. Characterization of the expression of the RNA binding protein eIF4G1 and its clinicopathological correlation with Serous Ovarian Cancer. *PLoS One* **11**, e0163447. <https://doi.org/10.1371/journal.pone.0163447> (2016).
- Hu, M. & Yang, J. Down-regulation of lncRNA UCA1 enhances radiosensitivity in prostate cancer by suppressing EIF4G1 expression via sponging miR-331-3p. *Cancer Cell Int.* **20**, 449. <https://doi.org/10.1186/s12935-020-01538-8> (2020).

24. Lu, Y. et al. Elevation of EIF4G1 promotes non-small cell lung cancer progression by activating mTOR signalling. *J. Cell. Mol. Med.* **25**, 2994–3005. <https://doi.org/10.1111/jcmm.16340> (2021).
25. Dell'Anno, I. et al. EIF4G1 and RAN as possible drivers for malignant pleural mesothelioma. *Int. J. Mol. Sci.* **21**, <https://doi.org/10.3390/ijms21144856> (2020).
26. Reyes-Turcu, F. E., Ventii, K. H. & Wilkinson, K. D. Regulation and cellular roles of ubiquitin-specific deubiquitinating enzymes. *Annu. Rev. Biochem.* **78**, 363–397. <https://doi.org/10.1146/annurev.biochem.78.082307.091526> (2009).
27. Bomberger, J. M., Barnaby, R. L. & Stanton, B. A. The deubiquitinating enzyme USP10 regulates the endocytic recycling of CFTR in airway epithelial cells. *Channels (Austin Tex)*. **4**, 150–154. <https://doi.org/10.4161/chan.4.3.11223> (2010).
28. Wilkinson, K. D. Ubiquitination and deubiquitination: targeting of proteins for degradation by the proteasome. *Semin. Cell Dev. Biol.* **11**, 141–148. <https://doi.org/10.1006/scdb.2000.0164> (2000).
29. Reed, B. J., Locke, M. N. & Gardner, R. G. A conserved deubiquitinating enzyme uses intrinsically disordered regions to Scaffold multiple protein Interaction sites. *J. Biol. Chem.* **290**, 20601–20612. <https://doi.org/10.1074/jbc.M115.650952> (2015).
30. Lawson, A. P. et al. Identification of deubiquitinase targets of isothiocyanates using SILAC-assisted quantitative mass spectrometry. *Oncotarget* **8**, 51296–51316. <https://doi.org/10.18632/oncotarget.17261> (2017).
31. Jung, Y. et al. Modulating cellular balance of Rps3 mono-ubiquitination by both Hel2 E3 ligase and Ubp3 deubiquitinase regulates protein quality control. *Exp. Mol. Med.* **49**, e390. <https://doi.org/10.1038/emm.2017.128> (2017).
32. Soncini, C., Berdo, I. & Draetta, G. Ras-GAP SH3 domain binding protein (G3BP) is a modulator of USP10, a novel human ubiquitin specific protease. *Oncogene* **20**, 3869–3879. <https://doi.org/10.1038/sj.onc.1204553> (2001).
33. Bomberger, J. M., Barnaby, R. L. & Stanton, B. A. The deubiquitinating enzyme USP10 regulates the post-endocytic sorting of cystic fibrosis transmembrane conductance regulator in airway epithelial cells. *J. Biol. Chem.* **284**, 18778–18789. <https://doi.org/10.1074/jbc.M109.001685> (2009).
34. Takahashi, M. et al. HTLV-1 tax oncoprotein stimulates ROS production and apoptosis in T cells by interacting with USP10. *Blood* **122**, 715–725. <https://doi.org/10.1182/blood-2013-03-493718> (2013).
35. Yuan, J., Luo, K., Zhang, L., Chevillat, J. C. & Lou, Z. USP10 regulates p53 localization and stability by deubiquitinating p53. *Cell* **140**, 384–396. <https://doi.org/10.1016/j.cell.2009.12.032> (2010).
36. Pan, L. et al. Deubiquitination and stabilization of T-bet by USP10. *Biochem. Biophys. Res. Commun.* **449**, 289–294. <https://doi.org/10.1016/j.bbrc.2014.05.037> (2014).
37. Lin, Z. et al. USP10 antagonizes c-Myc transcriptional activation through SIRT6 stabilization to suppress tumor formation. *Cell Rep.* **5**, 1639–1649. <https://doi.org/10.1016/j.celrep.2013.11.029> (2013).
38. Faus, H., Meyer, H. A., Huber, M., Bahr, I. & Haendler, B. The ubiquitin-specific protease USP10 modulates androgen receptor function. *Mol. Cell. Endocrinol.* **245**, 138–146. <https://doi.org/10.1016/j.mce.2005.11.011> (2005).
39. Liu, J. et al. Beclin1 controls the levels of p53 by regulating the deubiquitination activity of USP10 and USP13. *Cell*. **147**, 223–234. <https://doi.org/10.1016/j.cell.2011.08.037> (2011).
40. Draker, R., Sarcinella, E. & Cheung, P. USP10 deubiquitylates the histone variant H2A.Z and both are required for androgen receptor-mediated gene activation. *Nucleic Acids Res.* **39**, 3529–3542. <https://doi.org/10.1093/nar/gkq1352> (2011).
41. Guturi, K. K. N. et al. RNF168 and USP10 regulate topoisomerase II $\alpha$  function via opposing effects on its ubiquitylation. *Nat. Commun.* **7**, 12638. <https://doi.org/10.1038/ncomms12638> (2016).
42. Luo, Z. et al. A negative feedback regulatory loop between miR-138 and TP53 is mediated by USP10. *Oncotarget* **10**, 6288–6296. <https://doi.org/10.18632/oncotarget.27275> (2019).
43. Deng, S. et al. Over-expression of genes and proteins of ubiquitin specific peptidases (USPs) and proteasome subunits (PSs) in breast cancer tissue observed by the methods of RFDD-PCR and proteomics. *Breast Cancer Res. Treat.* **104**, 21–30. <https://doi.org/10.1007/s10549-006-9393-7> (2007).
44. Fotopoulou, C. et al. Outcomes of gynecologic cancer surgery during the COVID-19 pandemic: an international, multicenter, prospective CovidSurg-Gynecologic Oncology Cancer study. *Am. J. Obstet. Gynecol.* **227**, 735.e731-735.e725 <https://doi.org/10.1016/j.ajog.2022.06.052> (2022).
45. Zeng, Z. et al. Prognostic significance of USP10 as a tumor-associated marker in gastric carcinoma. *Tumour Biol.* **35**, 3845–3853. <https://doi.org/10.1007/s13277-013-1509-1> (2014).
46. Liu, H. et al. MicroRNA-191 promotes pancreatic cancer progression by targeting USP10. *Tumour Biol.* **35**, 12157–12163. <https://doi.org/10.1007/s13277-014-2521-9> (2014).
47. Liang, S. et al. Decreased expression of EIF4A1 after preoperative brachytherapy predicts better tumor-specific survival in cervical cancer. *Int. J. Gynecol. Cancer: Official J. Int. Gynecol. Cancer Soc.* **24**, 908–915. <https://doi.org/10.1097/igc.000000000000152> (2014).
48. Cromer, A. et al. Identification of genes associated with tumorigenesis and metastatic potential of hypopharyngeal cancer by microarray analysis. *Oncogene*. **23**, 2484–2498. <https://doi.org/10.1038/sj.onc.1207345> (2004).
49. Comtesse, N. et al. Frequent overexpression of the genes FXR1, CLAPM1 and EIF4G located on amplicon 3q26-27 in squamous cell carcinoma of the lung. *Int. J. Cancer*. **120**, 2538–2544. <https://doi.org/10.1002/ijc.22585> (2007).
50. Bach, P. et al. Computed tomography screening and lung cancer outcomes. *Rev. Portuguesa Pneumol.* **13**, 888–890. [https://doi.org/10.1016/s0873-2159\(15\)30384-6](https://doi.org/10.1016/s0873-2159(15)30384-6) (2007).
51. Yi, T., Kabha, E., Papadopoulos, E. & Wagner, G. 4EGI-1 targets breast cancer stem cells by selective inhibition of translation that persists in CSC maintenance, proliferation and metastasis. *Oncotarget*. **5**, 6028–6037. <https://doi.org/10.18632/oncotarget.2112> (2014).
52. Sanchez-Martin, M. & Ferrando, A. The NOTCH1-MYC highway toward T-cell acute lymphoblastic leukemia. *Blood*. **129**, 1124–1133. <https://doi.org/10.1182/blood-2016-09-692582> (2017).
53. Pickering, C. R. et al. Integrative genomic characterization of oral squamous cell carcinoma identifies frequent somatic drivers. *Cancer Discov.* **3**, 770–781. <https://doi.org/10.1158/2159-8290.Cd-12-0537> (2013).
54. Du, L., Li, J., Tian, Y. & Feng, R. Pleckstrin-2-promoted PPM1B degradation plays an important role in transforming growth factor- $\beta$ -induced breast cancer cell invasion and metastasis. *Cancer Sci.* **114**, 2429–2444. <https://doi.org/10.1111/cas.15791> (2023).
55. Liu, L. et al. Transforming growth factor Beta promotes inflammation and Tumorigenesis in Smad4-Deficient intestinal epithelium in a YAP-Dependent manner. *Adv. Sci. (Weinheim Baden-Wuerttemberg Germany)*. **10**, e2300708. <https://doi.org/10.1002/adv.202300708> (2023).
56. Liu, X., Chen, B., Chen, J., Su, Z. & Sun, S. Deubiquitinase ubiquitin-specific peptidase 10 maintains cysteine rich angiogenic inducer 61 expression via Yes1 associated transcriptional regulator to augment immune escape and metastasis of pancreatic adenocarcinoma. *Cancer Sci.* **113**, 1868–1879. <https://doi.org/10.1111/cas.15326> (2022).
57. Sango, J. et al. USP10 inhibits the dopamine-induced reactive oxygen species-dependent apoptosis of neuronal cells by stimulating the antioxidant Nrf2 activity. *J. Biol. Chem.* **298**, 101448. <https://doi.org/10.1016/j.jbc.2021.101448> (2022).
58. Li, P. et al. Stabilization of MOF (KAT8) by USP10 promotes esophageal squamous cell carcinoma proliferation and metastasis through epigenetic activation of ANXA2/Wnt signaling. *Oncogene* **43**, 899–917. <https://doi.org/10.1038/s41388-024-02955-z> (2024).

## Acknowledgements

We acknowledge our lab friends for their support. We also acknowledge assistance from medical writers, proof-

readers, and editors.

### Author contributions

FL designed this study. XY and RX collected and analyzed the data, and wrote the manuscript. DG and ZH assisted with cell culture and data analysis. XC, QS, and WZ helped with literature search and provided statistical guidance. YL and ZX supervised the study and reviewed the manuscript. All authors contributed to the article and approved the final version.

### Funding

This work was supported by a grant from the National Natural Science Foundation of China [grant number 81972183].

### Declarations

#### Ethics approval and consent to participate

Our study did not contain human participants, human data, or human tissue.

#### Competing interests

The authors declare no competing interests.

### Additional information

**Supplementary Information** The online version contains supplementary material available at <https://doi.org/10.1038/s41598-024-74490-6>.

**Correspondence** and requests for materials should be addressed to Y.L. or Z.X.

**Reprints and permissions information** is available at [www.nature.com/reprints](http://www.nature.com/reprints).

**Publisher's note** Springer Nature remains neutral with regard to jurisdictional claims in published maps and institutional affiliations.

**Open Access** This article is licensed under a Creative Commons Attribution-NonCommercial-NoDerivatives 4.0 International License, which permits any non-commercial use, sharing, distribution and reproduction in any medium or format, as long as you give appropriate credit to the original author(s) and the source, provide a link to the Creative Commons licence, and indicate if you modified the licensed material. You do not have permission under this licence to share adapted material derived from this article or parts of it. The images or other third party material in this article are included in the article's Creative Commons licence, unless indicated otherwise in a credit line to the material. If material is not included in the article's Creative Commons licence and your intended use is not permitted by statutory regulation or exceeds the permitted use, you will need to obtain permission directly from the copyright holder. To view a copy of this licence, visit <http://creativecommons.org/licenses/by-nc-nd/4.0/>.

© The Author(s) 2024